REVIEWS



The generation of large earthquakes

Aitaro Kato¹ Mand Yehuda Ben-Zion^{2,3}

Abstract | Despite decades of observational, laboratory and theoretical studies, the processes leading to large earthquake generation remain enigmatic. However, recent observations provide new promising perspectives that advance knowledge. Here, we review data on the initiation processes of large earthquakes and show that they are multiscale and diverse, involving localization of deformation, fault heterogeneities and variable local loading rate effects. Analyses of seismic and geodetic data reveal evidence for regional weakening by earthquake-induced rock damage and progressive localization of deformation around the eventual rupture zones a few years before some large earthquakes. The final phase of deformation localization includes, depending on conditions, a mixture of slow slip transients and foreshocks at multiple spatial and temporal scales. The evolution of slip on large, localized faults shows a step-like increase that might reflect stress loading by previous failures, which can produce larger dynamic slip, in contrast to the smooth acceleration expected for a growing aseismic nucleation phase. We propose an integrated model to explain the diversity of large earthquake generation from progressive volumetric deformation to localized slip, which motivates future near-fault seismic and geodetic studies with dense sensor networks and improved analysis techniques that can resolve multiscale processes.

How large earthquakes that break the entire brittle crust or significant sections of subduction zones (that is, events with Mw>7) are generated remains a fundamental unsolved scientific question, with substantial societal and economic importance. Large earthquakes, for example, can produce devastating destruction and loss of life, as illustrated by recent catastrophic earthquakes in Japan, Haiti and Indonesia, collectively producing over 500,000 fatalities and economic damage that may exceed US\$200 billion. Moreover, with increasing population density in seismically vulnerable major metropolitan areas such as Tokyo, Los Angeles, Mexico City and Istanbul, amongst others, there is a clear need to improve understanding of the processes that lead to large earthquakes.

Fundamentally, the initiation of large, dynamic rupture is linked to the evolution of stress and strength in a fault zone. Three main conceptual models (or frameworks) have been developed to explain the process¹-6 — cascade-up, pre-slip and progressive localization — each of which requires that the stress field is relatively high and correlated over large distances³-9. The cascade-up framework describes large earthquakes on a heterogeneous fault as occurring in response to static and dynamic stress perturbations induced by previous earthquakes, which add locally to the long-term tectonic stress¹0-12. In this model, earthquakes trigger a sequence of events on a set of pre-existing faults that culminate in large mainshock rupture⁴. The magnitude of the earthquake is unpredictable until the dynamic rupture has stopped⁵.

The pre-slip model, by contrast, outlines the generation of large events on a relatively homogeneous fault surface. These are initiated through an aseismic nucleation process involving slow slip or fluid movement that can trigger subsequent larger earthquakes¹³⁻¹⁵. As in the cascade-up framework, the pre-slip model is focused on processes that occur along a pre-existing large fault surface. This model is further underpinned by the assumption that tracking growing aseismic slip can be used as a sign of an imminent large earthquake. However, forecasting large earthquakes through monitoring prior aseismic slip has not yet been possible in natural settings³.

The progressive localization framework differs in that it does not focus on processes limited to pre-existing faults or sets of faults. Instead, it describes the progressive evolution from distributed failures in a rock volume to localized deformation, culminating in the generation of primary slip zones and large earthquakes^{2,6,16-18}. During the localization process, there are many clusters of seismicity in a zone containing multiple faults on different scales. Each cluster can have its own foreshocks^{19,20}, one of which might lead to the initiation of the mainshock rupture.

Indeed, foreshocks that occur close to subsequent larger events in space and time have often been used as indicators of imminent stress, slip or strength change in the source area^{21,22}, as they are the most obvious forerunner signal of the mainshock rupture. However, foreshocks can only be defined retrospectively through statistical analyses of seismic catalogues that include

¹Earthquake Research Institute, University of Tokyo, Tokuo, Japan.

²Department of Earth Sciences, University of Southern California, Los Angeles, CA, USA.

³Southern California Earthquake Center, University of Southern California, Los Angeles, CA, USA.

™e-mail: akato@ eri.u-tokyo.ac.jp https://doi.org/10.1038/ s43017-020-00108-w

Key points

- Progressive localization of shear deformation was observed before several Mw>7 shallow crustal earthquakes. Some mainshocks were also preceded by immediate foreshock sequences or slow slip.
- A step-like increase in fault slip driven by a combination of migrating slow slip transients and foreshocks occurred before some megathrust earthquakes in subduction zones. The intermittent increase in fault slip loads nearby locked regions, increasing the likelihood of subsequent large earthquakes.
- The initiation processes of large, natural earthquakes are diverse and include localization of deformation and complexities of subsequent slip, owing to strength heterogeneity, fault roughness and variable local loading-rate effects.
- Integrated, high-resolution seismic and geodetic observations, including additional near-fault sensors and advanced analysis techniques, are needed to improve the knowledge on the combination of aseismic slip and seismic sequences that lead to the occurrence of large, natural earthquakes.

the mainshocks^{19,20}. In addition, not every major earthquake is preceded by an observable nearby foreshock sequence^{3,23}. Nevertheless, recent precise earthquake catalogues show that some large earthquakes (along plate interfaces and in crustal fault systems) were preceded by an increased rate of seismicity in the months to days leading up to the mainshock^{22,24}.

In the cascade-up framework, foreshocks have an important influence, as they induce the dynamic rupture of the subsequent large earthquakes. By contrast, foreshocks in the pre-slip model are by-products of the underlying quasi-stable slip process, rather than directly responsible for triggering the mainshock. Thus, there has been debate regarding which model, cascade-up or pre-slip, is suitable for describing foreshock sequences in nature^{4,22,25,26}. In the progressive localization view, foreshocks of multiple clusters of events on different nearby faults are parts of a regional shear localization process that leads to large earthquakes⁶.

In this Review, we aim to resolve the debate regarding the generation of large earthquakes and the appropriateness or inadequacies of the three proposed frameworks. In particular, the cascade-up model has no consideration of aseismic slip and volumetric deformation; the pre-slip model has no consideration of stress perturbations from nearby earlier events and volumetric deformation; and the progressive localization model is less relevant or not relevant for systems dominated by an existing weak fault with little strength recovery. We examine how tectonic deformation and the evolution of fault behaviour are connected to the initiation processes of large earthquakes, primarily using recent seismic and geodetic monitoring in continental crust and subduction zone environments. We outline results on progressive localization of deformation, followed by discussion of well-documented case studies and fault slip before large ruptures. Based on geophysical observations, experiments and theoretical results, we propose an integrated model for the initiation of large earthquakes, and end with recommendations for future research.

Localization of deformation

Fault systems evolve with increasing total tectonic displacement, and the tectonic shear deformation gradually localizes onto major faults^{27,28}. During the initial stage

of fault development, tectonic strain is accommodated by pervasive deformation that can involve distributed cracking, discontinuities and geometrical heterogeneities such as stepovers, bends and conjugate faults. Interactions between weakening processes and the evolving fault system can promote the growth of large structures through fault linkage and coalescence^{2,18,29–31}.

Laboratory experiments with rock and analogue samples that are not dominated by large, pre-existing fault surfaces show that major ruptures are preceded by a relatively long phase of distributed deformation. At some level of deformation, the distributed deformation phase is followed by progressive shear localization, culminating in macroscopic instabilities along system-size fracture zones^{16,18,32,33}. Combined analyses of microfractures and temporal variations of seismic velocities in rocks show that low-velocity damage zones develop during the approach to the macroscopic failures^{34,35}. The transition from distributed deformation to shear localization before large events is also seen in results of numerical simulations with a damage rheology model^{36,37}. In such simulations, during the long interseismic periods, stress and strain build up in a broad region and produce distributed, small-scale ruptures that correspond to typical ongoing seismicity. Subsequently, during the localization phase, strain and seismicity become focused near a major fault zone, on which the next large earthquake occurs.

Localization of deformation in natural settings. Analysis of geodetic and seismic data documents progressive localization of deformation and an increasing rate of moderate to large earthquakes in the Western USA ³⁸. Events in an earthquake catalogue between 1996 and 2016 are strongly correlated spatially with the average strain rate from 1986 to 2012, as estimated by regional Global Navigation Satellite System (GNSS) network data. As a result, recent seismicity in the Western USA appears to be closely related to the strain rate and more localized around major tectonic boundaries, compared with data before the 1980s³⁸. Along the Japanese islands, there is also some correlation between historical large earthquakes and strain rates³⁹.

Rock damage generation and localization processes of ongoing, low-magnitude background seismicity have been examined quantitatively in relation to the occurrence of large earthquakes in Southern and Baja California^{6,40}. The results show that the Landers 1992 (Mw 7.3), Hector Mine 1999 (Mw 7.1), El Mayor-Cucapah 2010 (Mw 7.2) and Ridgecrest 2019 (Mw 7.1) earthquakes were preceded by generation of rock damage around the eventual rupture zones in the decades prior (FIG. 1). Furthermore, the ongoing seismicity around the impending rupture zones of the Mw>7 events became more localized and coalesced into larger clusters in the final 2-3 years before the mainshocks (FIG. 2). The examined large earthquakes are dominated by strikeslip faulting and are located in a complex, evolving transform plate boundary, where tectonic strain produces abundant ongoing seismicity40,41.

The concentrated generation of rock damage and shear localization before the occurrence of major earthquakes in Southern and Baja California support the

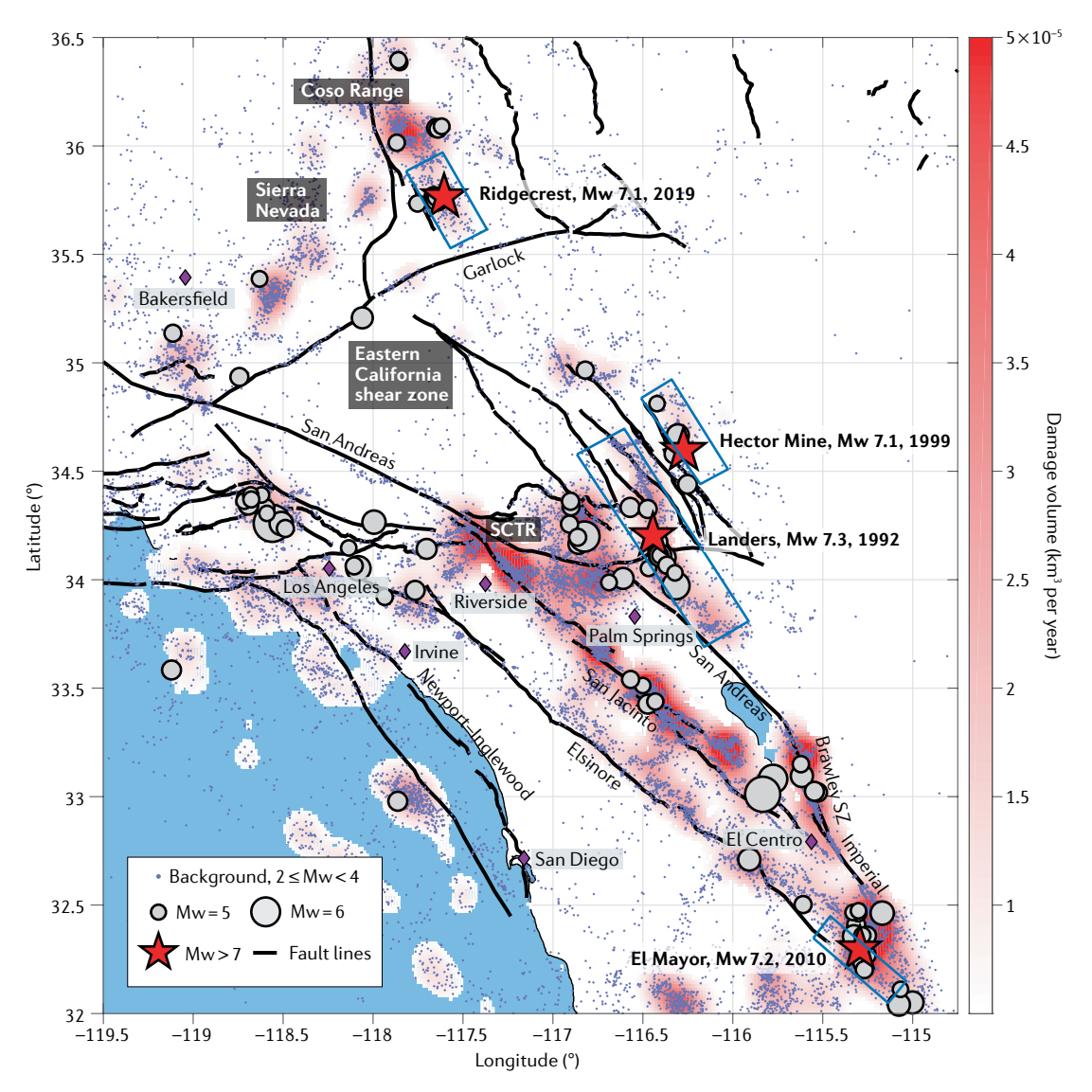
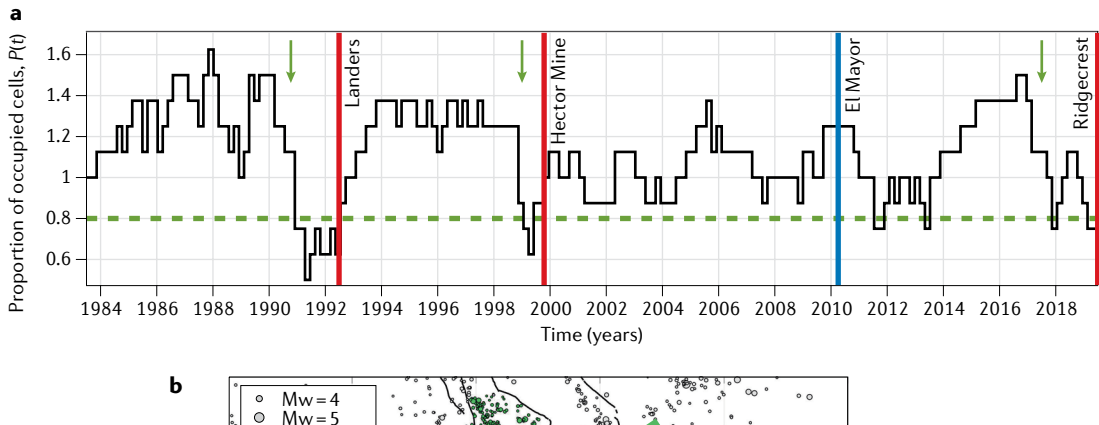
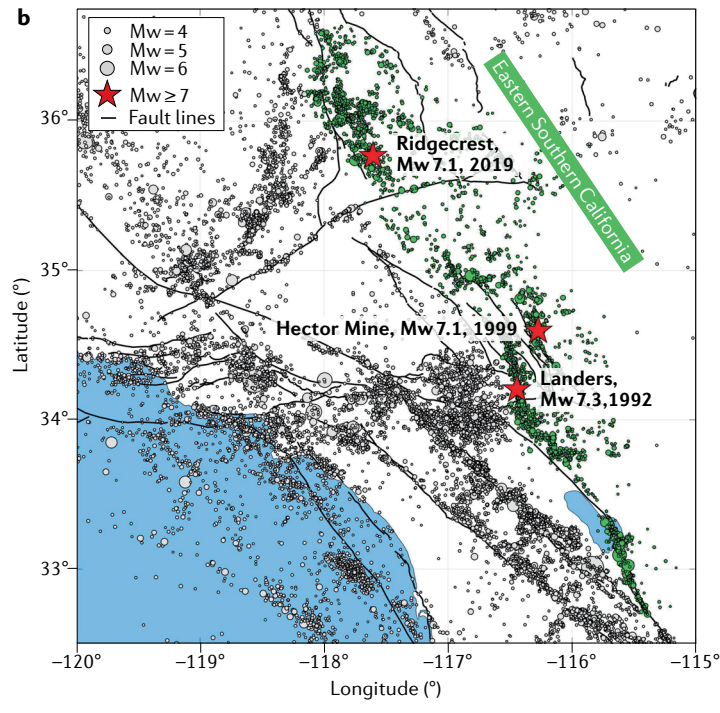


Fig. 1 | Generation of rock damage by background events around rupture zones of future large earthquakes. Estimated average annual production of rock damage volume (colour scale) by background earthquakes with magnitude $2 \le Mw < 4$ (dots) over January 1981–June 2019. The rock damage volume is estimated from the event magnitudes using scaling relations derived from earthquake phenomenology and fracture mechanics. The damage values are clipped at 5×10^{-5} km³ per year and values below 5×10^{-6} km³ per year are transparent. Damage volume is estimated using an updated earthquake catalogue of REF. and the background events are identified following REF. and REF. Earthquakes with Mw \ge 5, which are not used in the damage estimation, are shown for reference. Black lines mark major faults. The regions around the rupture zones of the June 1992 Mw 7.3 Landers, October 1999 Mw 7.1 Hector Mine, April 2010 Mw 7.2 El Mayor-Cucapah earthquake and July 2019 Mw 7.1 Ridgecrest earthquakes (blue rectangles) had considerable accumulation of rock damage prior to the occurrence of these events. Other areas with high rock-damage production by background events include the San Jacinto fault zone, the Brawley seismic zone (SZ) and the region around the South-Central Transverse Range (SCTR). Adapted and reprinted by permission of Oxford University Press on behalf of the Royal Astronomical Society, from REF. Ben-Zion, Y. & Zaliapin, I. Localization and coalescence of seismicity before large earthquakes. *Geophys. J. Int.* 223, 561–583 (2020).

progressive localization model. Specifically, the generation of rock damage appears to produce a progressive regional weakening, which enables a given hypocentre to become a large rupture, with its size outlined by the region of elevated rock damage. Progressive healing of rock damage can lead to partial recovery of strength during the deformation process^{42–44}. However, the recovery is only partial and continuing tectonic loading leads to episodic, large-scale re-localization of deformation.

Owing to insufficient near-fault data, the localization of shear strain before large events has not yet been substantiated by detailed geodetic measurements. Aseismic tectonic movements detected in geodetic data might also drive brittle deformation and can be used to define space—time regions in which to monitor the localization of seismicity. It is, therefore, highly important to continue to track spatial and temporal changes of strain rates by dense GNSS networks and analyses of interferometric





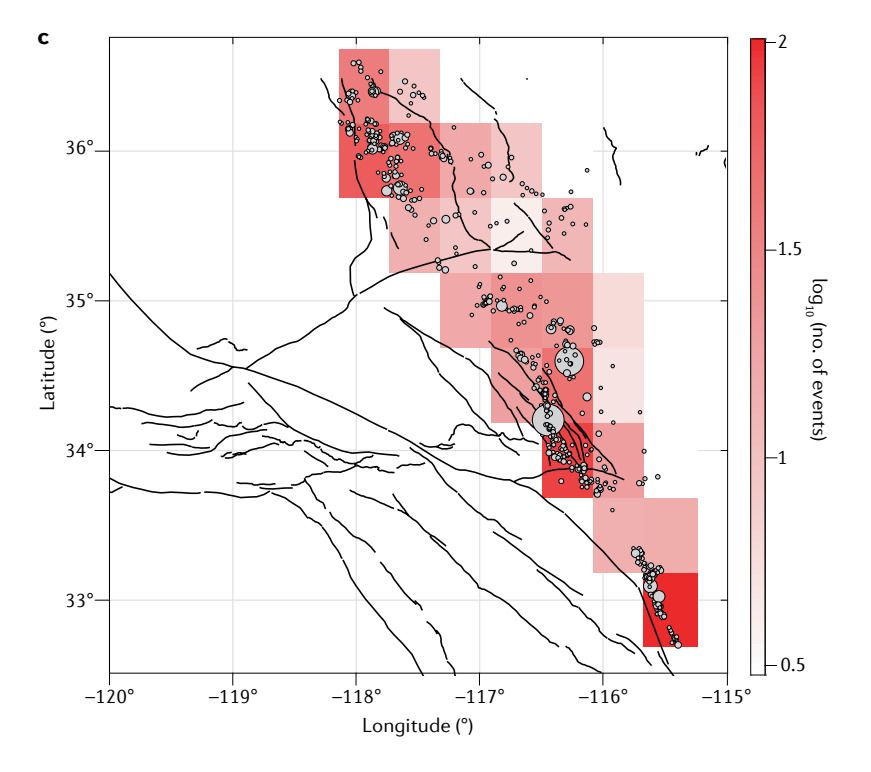


Fig. 2 | Localization of background events in eastern Southern California before Mw>7 earthquakes. a | Normalized proportion P(t) of active cells (black solid line). Red vertical lines indicate the times of the three largest (Mw>7) earthquakes in the region and the blue line denotes the El Mayor-Cucapah event in Baja California. The green arrows mark the initiation of significant reduction of P(t) prior to the three Mw>7 earthquakes and the green horizontal line highlights low values of P(t). In addition to three premonitory decreases before the Mw>7 events in the region, there is also a decrease after the El Mayor-Cucapah earthquake. b | Map of the examined background seismicity (green circles) in eastern Southern California. Other background events are shown by grey circles. c | Number of background events within cells of linear size of $\Delta \phi = 0.5^{\circ}$ in eastern Southern California. The normalized proportion P(t) of active cells (panel a) is the ratio of the number of cells that exceed the threshold $S_0 \Delta t / T$ with $S_0 = 20$ and sliding time window $\Delta t = 2.5$ years to the number of cells that exceed S_0 during the total examined time interval. Adapted and reprinted by permission of Oxford University Press on behalf of the Royal Astronomical Society, from REF.⁶, Ben-Zion, Y. & Zaliapin, I. Localization and coalescence of seismicity before large earthquakes. Geophys. J. Int. 223, 561-583 (2020).

synthetic aperture radar data. A separation of tectonic motion from surface loads and anthropogenic activity is needed to provide high-resolution results on slow crustal deformation⁴⁵.

Local triggering by seismic and aseismic slip. Along with the localization of seismicity, some foreshocks were observed closely before the three large, Mw > 7 earthquakes in Southern California 12,21,46,47, which contributed to the final stress transfer (less than 24h) around the mainshock hypocentres. The foreshocks preceding the Landers and Hector Mine earthquakes belong to swarm-type seismicity with low average stress drop, and their hypocentres migrate along the fault strike⁴⁶. Similar migration of a foreshock sequence with low stress drop was clearly observed before the 2014 Mw 6.2 Northern Nagano, Japan, earthquake at shallow crustal depth⁴⁸. On one hand, foreshock migration implies that they might be a product of aseismic transient deformation (slow slip or fluid movement) close to the mainshock hypocentres, which could support the pre-slip model. On the other hand, the immediate foreshocks before the Hector Mine earthquake have also been interpreted to be triggered by each other, in agreement with the cascade-up model¹². Both interpretations are associated with multiple uncertainties, starting with deciding which events are foreshocks, and that the location precision of some foreshocks is not sufficient to rule out that they occur on different subparallel faults. High-density, large-scale seismic arrays with about 1,000 stations over 400 km² have the potential to provide highly accurate hypocentre locations49. Such data combined with systematic determination of earthquake clusters and foreshocks 19,20 can result in better understanding of the driving forces of foreshock sequences.

Geodetic observations in central Kyushu, south-west Japan, where a series of powerful earthquakes occurred in 2016 at shallow crustal depths, support a slow slip transient during the foreshock sequence. Approximately 28 h after an initial Mw 6.2 earthquake, a mainshock of Mw 7.0 occurred close to the epicentre of the first event. The sequence of seismicity between the two major events shows a clear spatiotemporal evolution ⁵⁰. The events migrated along the fault strike to both the up-dip and down-dip sides of the foreshock zone.

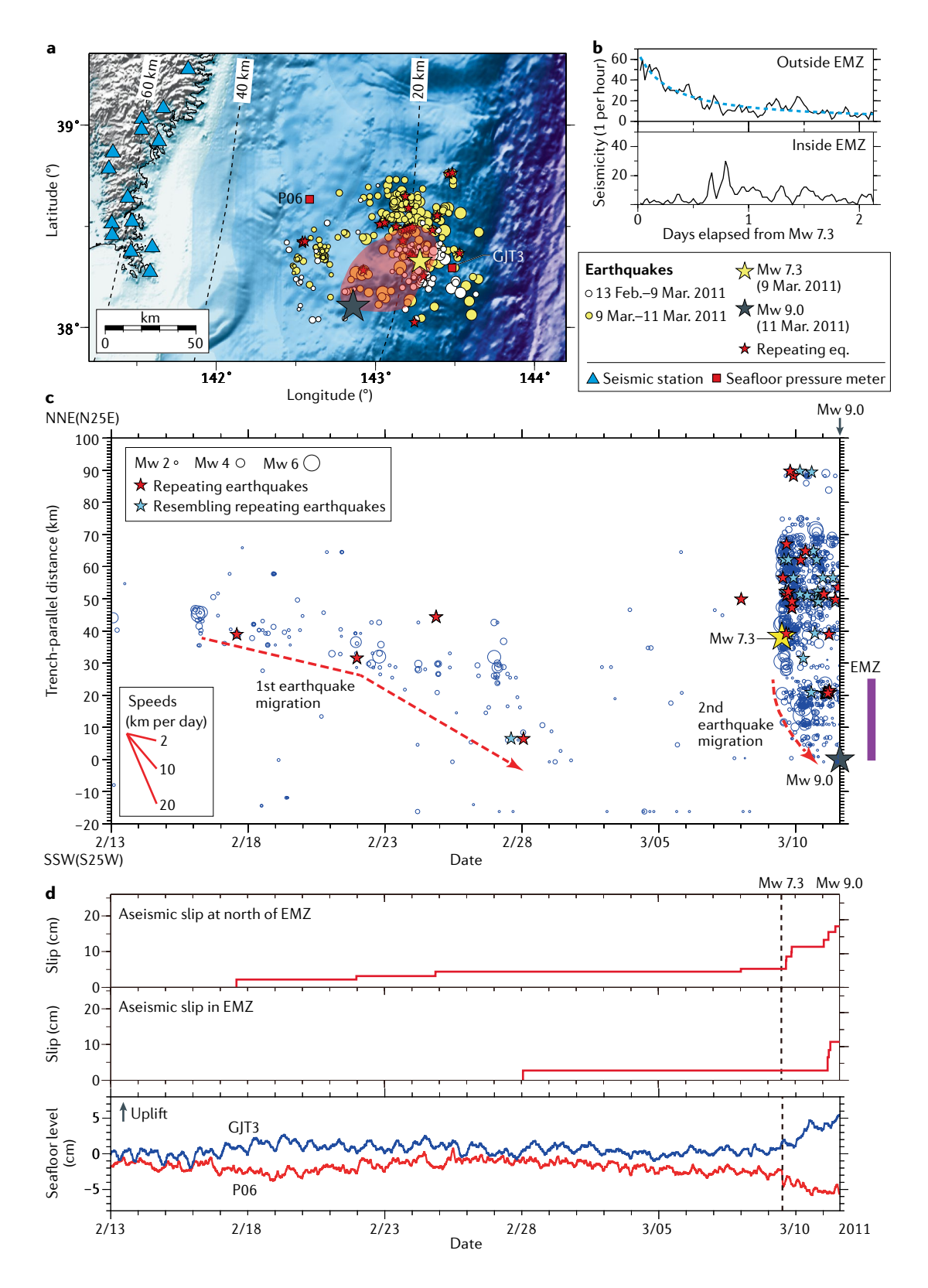
At the down-dip extension of the foreshock zone, the subsequent mainshock rupture initiated. Transient surface displacements following the Mw 6.2 foreshock were found using two GNSS stations close to the foreshock fault. The surface displacements can be explained by right-lateral slip on the foreshock fault, with an aseismic moment equivalent to Mw 5.8. It can, thus, be interpreted that the slow slip transient propagated towards the hypocentre of the mainshock rupture, contributing to the build-up of shear stress on the nearby mainshock hypocentre, together with stress changes induced by the foreshocks.

Seismic observations for a strike-slip fault system in central Alaska, USA, resolved simultaneous foreshocks and very low frequency (VLF) seismic radiation immediately before an earthquake of Mw 3.7 and depth of 17 km (REF. 15). The hypocentre was close to the brittleductile transition in the crust, and was preceded by a 12-h-long increase in foreshock activity. A rapid growth of foreshocks with 2-8-Hz waveforms was observed around 20 s before the onset of the mainshock rupture, and was coincident with the VLF waves (~0.05 Hz). The radiation of VLF waves is assumed to involve shear slip, with lower stress drops and slower rupture velocities than ordinary earthquakes, implying slow fault movement^{51,52}. The high-frequency waves of the immediate foreshocks were suggested to have radiated from the vicinity of an expanding slow slip front, interpreted as a nucleation process of the mainshock, as in the pre-slip model¹⁵. The temporal-amplitude growth of the foreshock waveforms appears to follow an exponential function, similar to the theoretical curve predicted for a relatively homogeneous fault⁵³. However, the foreshock waveforms are composed of multiple steps and do not follow a smooth acceleration, indicating a more complex process than in the pre-slip model. Alternatively, the intermittent increase in fault slip might have been caused by the combined occurrence of and interplay between the foreshock and slow slip.

Major subduction zone earthquakes

In subduction zones, shear deformation is highly localized along plate boundary faults that separate different lithological units and have very large total displacements through multiple seismic cycles. Thus, localization of deformation (and re-localization following partial healing in interseismic periods) might be less important for major subduction zone events compared with the crustal fault systems discussed previously. Here, we focus on the spatial and temporal evolution of localized slip along plate boundary faults in subduction zones.

A growing evidence of geophysical observations has demonstrated that subduction zone faults host a broad spectrum of slip modes, from slow slip to unstable fast slip, and produce a wide range of rupture behaviours^{54–56}. Tectonic stress can be released through both slow slip and fast slip modes, which can even occur on the same fault patch, owing to a temporal change in fault properties such as pore-fluid pressure⁵⁷. It is possible that both slow slip transients and unstable fast slip are involved during foreshock sequences and contribute to strength



weakening and stress loading of nearby segments, prompting subsequent dynamic ruptures. We devote particular attention to a few prominent foreshock sequences that can be explained by a step-like increase in slip caused by mixed modes of slow and fast slip that promote gradual unlocking of faults before major subduction events.

The 2011 Mw 9.0 Tohoku-Oki, Japan earthquake. Following the 2011 Mw 9.0 Tohoku-Oki earthquake, a step-like increase of slip along the plate boundary fault was documented before the megathrust rupture at multiple spatial and temporal scales⁵⁸⁻⁶³. The step-like increase of slip was shown in terms of seismicity, including foreshocks and deep intra slab

Fig. 3 | Step-like increase in fault slip before the 2011 Mw 9.0 Tohoku-Oki earthquake. a | Locations of the study area off Miyagi Prefecture and seismic stations (blue triangles). Black, yellow and red stars denote epicentres of the Tohoku-Oki mainshock, the largest foreshock (Mw 7.3) and the repeating earthquakes, respectively. Red shading represents the area with aseismic slip (>0.3 m) following the largest foreshock estimated by ocean-bottom pressure recorders⁶⁹ (red squares). White and yellow circles denote epicentres in the JMA catalogue between 13 February and 9 March, and between 9 March and 11 March 2011, respectively. **b** | Temporal changes in the rate of seismicity inside and outside the earthquake migration zone (EMZ) after the largest foreshock. The blue dashed curve denotes least-squares fitting of the modified Omori law. c | Spatiotemporal evolution of foreshocks (blue circles). Red dashed lines show approximate locations of earthquake migration fronts. Red stars denote repeating earthquakes and blue stars are identified to resemble repeating earthquakes. d | Average cumulative aseismic slip derived from repeating earthquakes in the two regional divisions (north of EMZ and within EMZ) and time series of seafloor changes measured by oceanbottom pressure records at GJT3 and P06 (REF.⁷⁰) (red squares in FIG. 3a). The black vertical dashed line marks the occurrence time of the largest foreshock. Adapted with permission from REF.58, AAAS.

earthquakes, crustal deformation and gravity field changes.

An intermittent increase in seismicity, which lasted for approximately one month, was observed at the northern side of the megathrust rupture initiation point along the plate boundary fault^{58,64} (FIG. 3a). A more precise earthquake catalogue, constructed by a template matching technique (FIG. 3b,c), shows that two sequences of foreshocks migrated along the trench-parallel direction towards the mainshock epicentre⁵⁸ (FIG. 3c). The migration speeds ranged from 2 to 10 km per day, comparable to those of episodic tremor and slow slip events observed along deeper extensions of strongly locked areas at warm subduction zones⁶⁵. In addition, the foreshock sequences included small repeating earthquakes, interpreted to result from recurrent rupture of seismic patches surrounded by aseismic creep on the plate interface⁶⁶⁻⁶⁸. Analysis of the earthquake migration with the repeating events suggests that the slow slip transient took place before the megathrust rupture, in the vicinity of the rupture initiation point.

During the final two days before the Tohoku-Oki earthquake, the slow slip transient was also documented by geodetic measurements using an on-shore GNSS network, as well as off-shore ocean bottom pressure records^{59,69,70}. The time series of geodetic data shows that the slow slip transient extended from the up-dip side of the coseismic slip zone, which hosted the largest foreshock (Mw 7.3 on March 9th 2011), towards the south (FIG. 3a,d), where the second migrating sequence of foreshocks showing swarm-type behaviour was observed (FIG. 3b). The equivalent magnitude of the slow slip transient ranges from 6.8 to 7.0. The time series of the geodetic data and the slip history derived from the repeating earthquakes indicate that the slow slip transient continued with a gradual decay of slip rate until the megathrust rupture (FIG. 3d). Seafloor measurements near the Japan Trench axis suggest that, between the middle of February 2011 and the onset of the largest Mw 7.3 foreshock, the slow slip transient was shallower than the largest foreshock rupture area and was accompanied by tectonic tremor^{60,71}. During this shallow slow slip transient, the first migrating foreshock sequence was also detected at greater depths⁵⁸.

Gravity-field variations along the Japanese arc from Gravity Recovery And Climate Experiment (GRACE) satellite data⁶³ were identified in the months preceding the Tohoku-Oki earthquake, although the statistical significance of the variations is disputed⁷². Assuming that the increase in the gradient of the gravity anomaly is valid, it implies that an aseismic extension of the Pacific-plate slab occurred at mid-upper mantle depths (namely, a slab plunge). The slab deformation was concomitant with increasing seismicity in the shallower slab, including the foreshock activity, and with a rise of extensional mechanisms deeper than 50 km (REE.⁷³). Deep slab deformation might cause stress loading in the region that underwent shallow foreshock sequences and slow slip transients⁶¹.

On decadal scales, on-land GNSS networks have revealed long-term aseismic creep on the plate interface along the down-dip and south area of the large coseismic slip zone of the Tohoku-Oki rupture^{62,74,75}. The aseismic creep appears to have started around 2005 and continued until the Tohoku-Oki mainshock. The total moment of the deep, long-term creep increased gradually until the time of the mainshock, finally reaching an equivalent magnitude of Mw 7.7. In addition, analyses of repeating earthquakes and VLF earthquakes off Tohoku reveal that seismic activity south of the Tohoku-Oki rupture area has slightly increased since 2008 (REFS^{52,76,77}). These observations suggest that long-term aseismic creep led to an increase in the stress rate on locked parts of the megathrust over decadal scales. The increased stress rate might have promoted moderate to large earthquakes off the Tohoku region after 2003 (REF. 78). However, with the limited available geodetic data, it is unclear whether the long-term creep occurred in connection with the Tohoku-Oki earthquake or as a temporal fluctuation of the locked state along the plate-boundary fault in interseismic periods.

The 2014 Mw 8.2 Iquique, Chile earthquake. A step-like evolution of seismicity and crustal deformation occurred during the 2014 Mw 8.2 northern Chile earthquake (FIG. 4a). The most striking features of the pre-rupture period were intense foreshock sequences and geodetic signals, which lasted for at least two weeks prior to the megathrust^{79–81}. Intense seismic bursts, including some Mw 6+ earthquakes, migrated at speeds of ~2−10 km per day along the fault dip and strike (FIG. 4b). A step-like increase in aseismic slip during the migrating sequences was derived from analyses of repeating earthquakes and the background rate of seismicity $^{81\text{--}83}$ (FIG. 4c). At the same time, the GNSS stations located along the coast near the source region started to move trench-ward, implying a gradual unlocking of the plate boundary fault^{80,81}. It has been debated whether the unlocking of the plate interface was driven mainly by slow slip or cumulative seismic slip from Mw 5-6-class foreshocks^{80,81,84}. This uncertainty arises from the weak signal of detected surface deformations that cannot be clearly separated into coseismic and aseismic slip^{80,81}. However, analyses of GNSS data85 and repeating earthquakes82,83 suggest that a slow slip transient occurred at the up-dip side of the main ruptured area during the final 17 days prior to

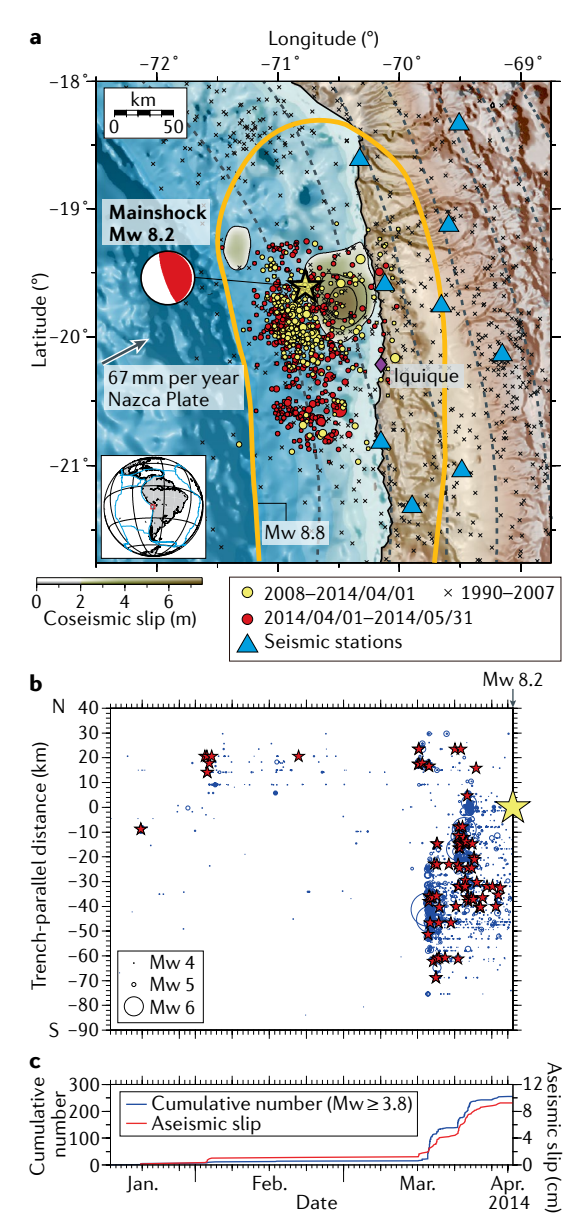


Fig. 4 | Step-like increase in fault slip before the 2014 Iquique, Chile Mw 8.2 earthquake. a Tectonic map of northern Chile. The yellow star denotes the epicentre of the mainshock rupture, with the moment tensor solution by the US Geological Survey. The colour scale and black contour lines show the coseismic-slip distribution estimated by teleseismic waveform inversion¹⁴⁹. Yellow and red circles are epicentres before and after the mainshock, respectively. Crosses show US Geological Survey catalogue epicentres from 1990 to 2007. The yellow outline denotes the approximate rupture area of the 1877 Mw 8.8 earthquake. Blue triangles are seismic stations. The inset shows the location of the study region. **b** | Space-time diagram of the foreshocks (blue circles) and repeating earthquakes (red stars), from monthly to daily timescales (blue circles scaled to magnitude). Yellow star denotes the hypocentre of the mainshock. c | Observed cumulative number of earthquakes with magnitude ≥3.8 (blue curve), and averaged aseismic slip inferred from repeating earthquakes (red curve). Adapted from REF.83, CC BY 4.0.

the mainshock (FIG. 4b,c). The equivalent moment magnitude released by the slow-slip transient was estimated to be \sim 6.6–6.8 (REFS^{82,83}).

A few months before the megathrust rupture, seismic activities at the southern and northern parts of the rupture area initiated at the up-dip side of the mainshock rupture 79 (FIG. 4b). The shallow seismicity occurred synchronously with bursts of deep earthquakes (>100 km) in the subducting slab 73,86 . The extensional mechanisms of the deep shocks imply that the slab was stretched at depth and plunged to the mantle, as observed before the 2011 Tohoku-Oki earthquake, Japan.

Long-term seismicity since 2008 in the region of the Mw 8.2 earthquake reveals that the step-like increase in seismicity, growing aseismic slip and increasing background seismicity rate started up-dip of the largest coseismic slip patch, about 8 months before the mainshock. Repetitive sequences of migrating slow slip events occurred along dip as well as along the fault strike, outlining the shallow rim of the largest coseismic slip patch⁸³. These signals might reflect the localization of shear deformation, as observed for the large crustal earthquakes discussed earlier. Furthermore, a long-term slow slip event with Mw 6.5, which was active from 8 months to 2 weeks before the mainshock (from July 2013 to middle of March 2014), has been identified on the southern side of the mainshock rupture in GNSS signals⁸⁷. The combination of the preceding seismicity and geodetic signal suggests that the fault slip accelerated in a step-like fashion.

Other examples of step-like increase in fault slip before large earthquakes. A step-like increase in fault slip along the subducting plate boundary was also observed during the foreshock sequence prior to the 2017 Valparaíso Mw 6.9 earthquake in Central Chile (at the northern extension of the rupture area of the 2010 Maule Mw 8.8 earthquake)88 and the 2008 Ibaraki-Oki earthquake (Mw 6.9) in Japan⁸⁹. Consistent with the earlier examples, slow slip transients prior to each earthquake were accompanied by intensive foreshocks migrating towards the mainshock hypocentre in the seismogenic zone. The migrating slow slip transients and foreshocks likely occurred near the edge of the strongly locked zone along the subduction plate boundary83,87, implying that the accumulated elastic strain along the plate interface was partially released by mixed modes of both slow and fast slip at multiple spatial and temporal scales before several large earthquakes. Note, the strain release typically progresses in a stepwise manner with time, rather than smoothly until the mainshock rupture^{83,87}, and that the energy flux can have important effects on the generated slip modes90. Faults can sustain short slip episodes separated by stuck periods causing intermittent movements91 and an intermittent increase in fault slip can load strongly locked parts nearby, increasing the likelihood of a subsequent large earthquake rupture.

Triggering of earthquakes by recurrent slow slip events. Since roughly the year 2000, recurrent slow slip events have been detected along global subduction zones at partially coupled areas, such as shallower and deeper

extensions of the strongly locked seismogenic zone^{55,92-94}. Further resolving the relationship between slow slip events and large, damaging earthquakes remains an important challenge^{55,56,93,95}. Episodic stress transfer from recurrent slow slip events to the adjacent megathrust faults increases the probability of triggering large earthquakes^{96,97}. However, many slow slip events do not lead directly to major seismic events. Although slow slip events load the adjacent locked patch, generation of large, dynamic rupture depends on the areal extent of the fault and proximity to failure^{55,97}.

Several observations indicate various interactions between slow slip events and regular earthquakes. Along the subduction zones in Mexico and Costa Rica, for example, Mw ~7-class earthquakes occurred during repetitive slow slip events $^{98-100}$. At the down-dip extension of the Guerrero section in Mexico, recurrent large-scale, slow slip events (with moment equivalent about Mw 7.5) have been observed approximately every 4 years, and the Mw 7.3 Papanoa (Mexico) earthquake took place in 2014 during the early stage of a long-term slow slip event (Mw 7.6) 100 . The slow slip event had an equivalent moment of Mw 7.1 at the onset of the Papanoa earthquake and the spatial closeness suggests that the Papanoa earthquake was triggered by the slow slip event 100 .

There have been several other direct observations connecting shallow slow slip events and regular moderate earthquakes. Shallow slow slip events along subduction zones in Japan, New Zealand and Ecuador were often accompanied by substantially increased levels of seismicity^{101–103}. In all these cases, the shallow slow slip events lasted less than a few weeks and occurred on a plate interface with heterogeneous interseismic coupling⁹³.

In addition, near the eastern coast of Boso Peninsula, central Japan, multiple slow-slip events with Mw ~6.6 occur every 4-7 years along the top of the subducting Philippine Sea Plate and are accompanied by seismic swarms at the down-dip edge of the major slow slip patch (with Mw 5.3 being the largest recorded earthquake). The seismicity clearly migrated from offshore to the coast, tracking the propagation of the slow slip front 104,105 (FIG. 5). Correlations in space and time between slow slip and seismicity suggest that the earthquake swarms are triggered by stress changes from the slow slip. Furthermore, an elaborate analysis of the GNSS data for the 1996 and 2013-2014 Boso slow slip events reveals that each event grew silently, with migration of the slip front without any detectable seismicity^{105,106} (FIG. 5). In such cases, the slow slip preceded the seismicity and increased the loading rates on the brittle patches over the plate interface. As discussed next, the local increase in the loading rate induced by the early slow slip contributes to the initiation of brittle failure. Detection of slow slip episodes might, thus, be used to identify increased likelihood of approaching large earthquakes.

Transition from aseismic to seismic fault behaviour. Based on seismicity analysis, it has been reported that, immediately after the 2011 Tohoku-Oki earthquake, a previously unrecognized slow slip event was triggered offshore of the Boso Peninsula¹⁰⁷. The triggered slow

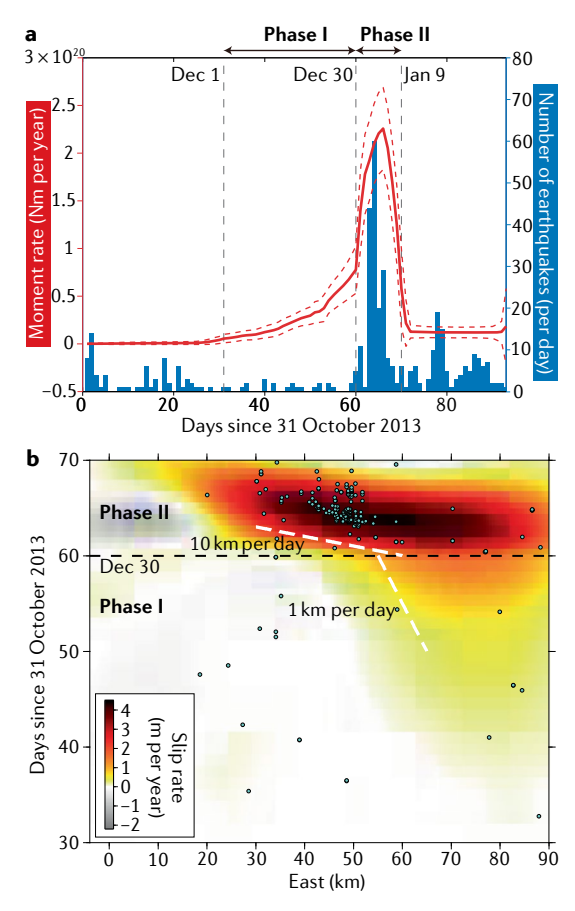


Fig. 5 | The 2013–2014 Boso slow slip event. a | Momentrate function (solid red line) calculated from the estimated fault slip rate with a rigidity of 30 GPa. Red dashed lines represent the error bounds (one standard deviation). The blue vertical bars denote the number of earthquakes per day. b | Temporal evolution of slip rate projected along 35.26°N latitude (shading). Blue circles are earthquakes detected by the template-matching technique. The horizontal axis represents the east-west distance measured from (140.0°E, 35.26°N). White dashed lines denote slopes corresponding to propagation speeds of 1 and 10 km per day. Reprinted with permission from REF. 106, Wiley.

slip event had a shorter duration and faster migration speed among the numerous known slow slip events¹⁰¹. Static and dynamic stress transfer by the Tohoku-Oki earthquake and the subsequent rapid afterslip¹⁰⁸ caused higher loading rate on the fault, promoting a faster slip rate that made the fault patch more brittle.

There are several additional examples of slip instability caused by rapid changes in loading rate. For example, rapid loading induced by the afterslip following the 2011 Tohoku-Oki earthquake likely caused the slip style of the repeating earthquakes to be more brittle. In addition, both the peak coseismic slip and the source dimension of a repetitive Mw $\sim\!\!5$ Kamaishi-oki earthquake demonstrate a positive correlation with the slip rate of the afterslip near the source area 109 . Thus, the faster the loading rate by the early afterslip, the larger the source dimensions of the repetitive earthquakes.

The rate-dependent slip behaviour can be explained by a conditionally stable frictional regime on the

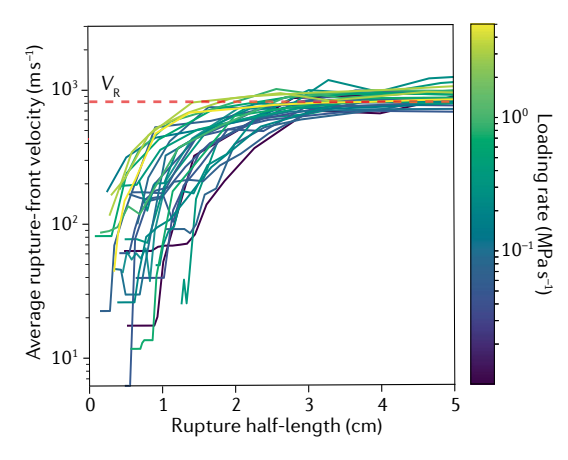


Fig. 6 | Characteristics of the nucleation phase for individual ruptures under different background loading rates in laboratory experiments. The average rupture-front velocity at each time step as a function of the rupture length. Bright colours represent higher loading rates. The horizontal dashed line denotes the Rayleigh-wave velocity of the medium ($V_{\rm p}$). Adapted from REF. ¹¹², CC BY 4.0.

associated plate boundary fault sections¹¹⁰⁻¹¹². The evolution of shear stress on the plate interface during the Tohoku-Oki afterslip is found to be consistent with rate-dependent frictional properties that might enhance instability as the slip rate increases, approaching the conditionally stable frictional regime¹⁰⁸. It is also well known that ductile rheologies can become brittle with increasing loading rate, which is likely responsible for transient deepening of the brittle–ductile transition depth in crustal faults¹¹³⁻¹¹⁵ and might play an important role in generating earthquakes in the nominally ductile lower crust¹¹⁶.

As shown in various laboratory experiments (FIG. 6), increasing the loading rate can also change the slip stability by reducing the nucleation length required to trigger unstable slip^{90,112,117-119}. This loading rate effect is qualitatively consistent with features predicted by a numerical model⁵³, and implies that, as the loading rate increases, the nucleation length can become shorter than the size of the brittle patch, leading to dynamic rupture. The reduction of nucleation length is consistently observed during experiments at a variety of stress levels120, and it might be linked to a self-organized, evolving structure within the fault gouge layer during shearing¹¹⁹. Higher loading rates produce more fault gouge, resulting in heterogeneous fault zones, which can have significant implications for nucleation length 121,122 and frictional slip instability^{123,124}. The size of the nucleation process affects the final triggering of earthquake ruptures and is complementary to the regional damage weakening process discussed for crustal earthquakes.

Fault slip before large ruptures

In laboratory experiments with relatively smooth surfaces, the slip smoothly increases as a function of time to failure during the nucleation stage, according to a power law or an exponential-type relation^{122,125}. Such behaviour has been demonstrated for different experimental conditions and materials, and has also been simulated in

various models of frictional faults $^{126-128}$. The accelerating fault slip observed in laboratory experiments is almost all aseismic (>~98%) 129 , but loads brittle patches and sometimes produces foreshock acoustic emission. The rate of foreshock acoustic emission is correlated with aseismic slip propagation during the nucleation stage of the experiments, and accelerates as the mainshock is approached 130,131 .

As discussed previously, seismic and geodetic observations show that fault slip does not accelerate smoothly, but increases in a step-like manner during foreshock sequences on subduction zones. Even during the clear foreshock sequence observed before the 2014 Chile Iquique earthquake, several steps are observed in the aseismic slip estimated from repeating earthquakes⁸³, in contrast to the smooth acceleration observed in laboratory experiments with relatively homogenous surfaces. In addition, the rate of surface displacements obtained by the GNSS network shows a gradual decay with time, instead of a smooth acceleration above the noise level^{80,85,87}.

Similarly, before the 2011 Tohoku-Oki earthquake, the slow slip transient continued with a gradual decay and no smooth slip acceleration before the mainshock⁷⁰ (above the detection threshold of ocean bottom pressure recorders with minimum observable slow slip of Mw \sim 6.0–6.2) (FIG. 3d). Furthermore, a waveform analysis of the initial onset of the 2011 Tohoku-Oki earthquake reveals that the beginning of the dynamic rupture was likely a small earthquake of Mw 4.9 (REF. 132). Both observations suggest that the moment released by the short-term nucleation process (that is, the final acceleration phase) is smaller than that expected from a scaling of the nucleation length based on a fracture mechanics approach¹³³. In addition, the ratio of the moment released by slow-to-fast (seismic) slip during the natural foreshock sequence^{58,83} (<~40%) is smaller than that observed in laboratory experiments during the nucleation phase¹²⁹ (>98%). As such, the experimental foreshock sequences are more aseismic than those observed in nature. Therefore, natural faults appear to be more brittle with higher susceptibility to dynamic rupture compared with the machined laboratory surfaces with simple geometry and less off-fault damage.

Given the complexity of natural fault structures, it is more appropriate to consider models where multiscale patches are incorporated in a rate-dependent frictional fault134-136. In a heterogeneous fault model, with a large strong patch containing smaller fragile patches, two different critical nucleation length scales are present on the same fault surface¹³⁶. In this model, a break of the small seismic patch (with a short nucleation length) can produce a small seismic event that might induce subsequent dynamic rupture in the surrounding fault and cause larger ruptures without a large size nucleation. Such a cascade-up rupture growth circumvents the larger nucleation process that corresponds to the larger strong patch and produces a small and negligible nucleation length that might be too difficult to observe from the surface. It would be useful to expand this model to include multiscale hierarchical structure, fault roughness and local loading-rate effects on nucleation sizes observed in recent experiments^{119,120}. Such models and more general damage-rheology frameworks with fault structures that evolve during the occurrence of ruptures^{137,138} might be able to quantitatively explain the diversity of slip modes and foreshocks observed along major subduction zones, including an intermittent increase in fault slip without any detectable smooth acceleration immediately before a major event.

Integrated earthquake generation model

Natural fault zones have hierarchical structures and considerable strength and stress variations along the main fault surfaces³. Three different models — cascade-up, pre-slip and progressive localization — were developed to explain the initiation process of large earthquakes. The three models consider different faulting environments (heterogeneous pre-existing faults, a smooth preexisting fault surface and volumetric deformation with evolving fault structures, respectively), and they address different spatial-temporal scales focusing on different characteristic phenomena. We propose an integrated model that can explain the diversity of processes leading to large earthquakes in different tectonic settings (FIG. 7). First, a general view of natural faulting should consider rock volumes rather than individual surfaces. Consideration of rock volumes is especially important in complex crustal fault systems, but is also relevant for subduction zones and major continental plate boundary faults. Laboratory experiments 44,139,140 and field observations¹⁴¹⁻¹⁴³ indicate that faulted materials regain frictional strength and cohesion rapidly after failure. The strength recovery necessitates some form of re-localization of deformation to the main fault zones at the end of the long interseismic periods, as part of a regional preparation process of subsequent major earthquakes. The re-localization of deformation is expected to be less pronounced, and more rapid, in geometrically simple sections of large faults compared with disordered fault structures, although it might have important manifestations also in relatively simple structures, including subduction zones.

In complex crustal faults, large earthquakes are preceded by progressive generation of elevated rock

damage by the ongoing seismicity around the eventual rupture zones (FIG. 7a). Foreshocks occur as part of seismic clusters and are simultaneous with possible aseismic deformation as shear localization proceeds (FIG. 7b). One foreshock sequence can trigger (with possible aseismic deformation) the large dynamic rupture along the main fault zone. In subduction zones, which are characterized by relatively high temperatures and abundant fluids, the final preparation phase leading to large earthquakes appears to be driven by a mixture of slow-slip transients and foreshocks (FIG. 7c).

Crustal faults are generally associated with colder and drier environments compared with subduction zones, so slow slip transients are less common. In addition, owing to the higher temperature, abundant fluids and involvement of slow slip transients, foreshocks in subduction zones are likely to be more frequent compared with those in crustal settings²². The migration of slow slip transients contributes to the build-up of shear stress on mainshock hypocentre sites, along with stress changes induced by foreshock ruptures.

When a strong, small patch on a fault breaks, it produces a rapid local increase in the loading rate around the patch, which can make the surrounding fault more brittle and susceptible to dynamic rupture. Foreshocks on a relatively smooth surface can be explained by ruptures of small fragile patches, which may be triggered by slow slip that can also jump-start a much larger rupture (that is, a 'rate-dependent cascade-up model')¹²⁰, which connects the cascade-up and pre-slip models¹³⁶. Yet, the rate-dependent cascade-up model still assumes smoothly accelerating slow slip that drives the system immediately before the dynamic rupture. However, as outlined previously, detailed observations show an intermittent, step-like behaviour of fault slip during the final foreshock sequence, rather than a smooth accelerating slip before the main rupture (FIG. 7c). Intermittent slip by a combination of slow and fast failure modes increases the stress on the eventual rupture zone and produces local variations of loading rates that modify the effective frictional behaviour of different fault sections118,119.

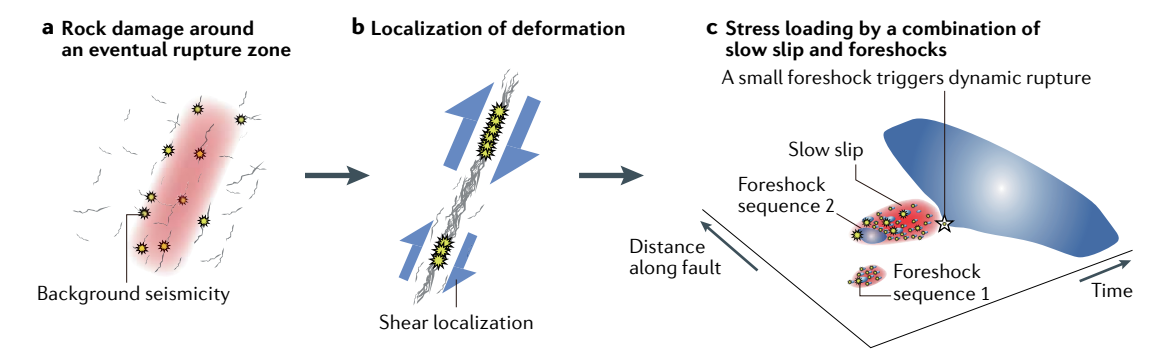


Fig. 7 | Schematic illustrations of generation processes of large earthquakes. a | Progressive localization of shear deformation and background seismicity around a large rupture zone. b | Shear localization and several foreshock sequences before the instability leading to the large rupture. c | A space—time diagram of step-like increase in fault slip before a major earthquake associated with combined slow slip and foreshocks. A final rapid local loading by a small foreshock triggers the subsequent major dynamic rupture and circumvents the large nucleation process of a large patch. White and yellow stars denote epicentres of mainshocks and other events, respectively. As an example, two foreshock sequences accompanied with slow slip are displayed.

Most seismic activities, swarms and slow slip events do not produce large earthquakes. The occurrence of large ruptures requires that the stress field generated by the tectonic loading and the combined stress transfers from various earlier failures is relatively high and correlated over a large portion of the fault^{7–9}. When the evolving stress is sufficiently close to the strength on a localized fault surface over a large area, one small (foreshock) event finally triggers a large dynamic rupture (FIG. 7c).

Summary and future perspectives

Generation of large earthquakes includes complex, multiscale processes that might have various dominant features in different tectonic environments. Shallow crustal earthquakes often occur in heterogeneous fault systems. Analyses of seismic and geodetic data show several manifestations of progressive localization of deformation before Mw > 7 crustal earthquakes, in agreement with laboratory fracturing experiments and damage rheology models. The observations include generation of rock damage by ongoing seismicity around future rupture zones, which produces crustal weakening on a decadal scale, and localization of background seismicity and coalescence of events into growing clusters in the final ~2-3 years before the large earthquakes. In some cases, it is possible to identify immediate foreshock sequences with spatial migration towards the mainshock hypocentre and lower stress drop in the final localization stage. The migrating foreshocks indicate that there might be some involvement of slow slip transients, although supporting geodetic measurements remain rare for shallow crustal environments. Improving the acquisition and analyses of observations can allow crustal deformation to be tracked from progressive localization to precursory foreshocks and slow slip transients before large crustal earthquakes. In particular, it is essential to close the critical data gap of insufficient near-fault recordings, since far-field observations do not provide detailed information about the faulting process144.

In subduction zones, major faults with a relatively simple geometry might have a weaker re-localization of deformation prior to large events compared with crustal faults. Intermittent fault slip is observed before some megathrust earthquakes at multiple spatial and temporal scales. Foreshocks tend to migrate towards the mainshock hypocentre, as seen for some shallow, large crustal earthquakes, and are accompanied by slow slip transients that likely occur near the edges of strongly

locked subduction zone faults. The evolution of fault slip on major subduction zone faults shows a step-like increase that is likely driven by a combination of slow slip and foreshocks. Such observations are not consistent with a gradual acceleration of fault slip, which is expected for the simple nucleation phase based on laboratory friction experiments and models of smooth fault surfaces. Natural faults appear to slip and stick quickly, causing intermittent movements, which reflect multiple failures on heterogeneous faults that finally trigger large dynamic ruptures.

Results from frictional experiments on the reduced size and duration of nucleation phases with increasing loading rate, and from numerical simulations on small-scale failure inducing larger dynamic rupture without a larger slow-nucleation process, can help explain the observed intermittent slip. Understanding how to scale the laboratory results to conditions representative of natural faults (that is, hierarchical heterogeneous systems that are subjected to multiple loads and varying boundary conditions), and using corresponding computer models to conduct numerical experiments on evolving earthquakes and faults over space scales and timescales not available for laboratory and field studies, can provide key additional contributions.

Improved understanding of the preparation processes leading to large earthquakes, and corresponding near-real-time monitoring of crustal deformation with seismic and geodetic data, will contribute to mitigation of seismic risk. Such efforts require high-resolution, near-field observations, along with laboratory experiments and models that account for localization of shear deformation and evolution of fault slip before major rupture. Dense near-fault arrays with co-located accelerometers, broadband seismic stations and high-rate geodetic sensors will be able to record ground motion over a wide range of amplitudes and frequencies. Such arrays, augmented by distributed acoustic sensors and other geophysical instruments, will be able to monitor deformation in the period leading to large earthquakes (including switching from slow deformation to fast slip) in sufficient detail to recover the physical processes that occur within rupture zones. Analysing field and laboratory data with artificial intelligence and other advanced methods can maximize the information extracted from the data and improve the predictive power that can be obtained from the available observations^{145–147}.

Published online 17 November 2020

- Fukao, Y. & Furumoto, M. Hierarchy in earthquake size distribution. *Phys. Earth Planet. Inter.* 37, 149–168 (1985).
- Reches, Z. & Lockner, D. A. Nucleation and growth of faults in brittle rocks. J. Geophys. Res. 99, 18159–18173 (1994).
- Ben-Zion, Y. Collective behavior of earthquakes and faults. *Rev. Geophys.* 46, RG4006 (2008).
- Gomberg, J. Unsettled earthquake nucleation. Nat. Geosci. 11, 463–464 (2018).
- Abercrombie, R. E. Similar starts for small and large earthquakes. *Nature* 573, 42–43 (2019).
- Ben-Zion, Y. & Zaliapin, I. Localization and coalescence of seismicity before large earthquakes. *Geophys. J. Int.* 223, 561–583 (2020).
- Ben-Zion, Y. Stress, slip, and earthquakes in models of complex single-fault systems incorporating brittle and

- creep deformations. J. Geophys. Res. Solid Earth 101, 5677–5706 (1996).
- Sammis, C. G. & Smith, S. W. Seismic cycles and the evolution of stress correlation in cellular automaton models of finite fault networks. *Pure Appl. Geophys.* 155, 307–334 (1999).
- Ben-Zion, Y., Eneva, M. & Liu, Y. Large earthquake cycles and intermittent criticality on heterogeneous faults due to evolving stress and seismicity. J. Geophys Res. Solid Earth 108, 2307 (2003).
- Ellsworth, W. L. & Bulut, F. Nucleation of the 1999 Izmit earthquake by a triggered cascade of foreshocks Nat. Geosci. 11, 531–535 (2018).
- Ide, S. Frequent observations of identical onsets of large and small earthquakes. *Nature* 573, 112–116 (2019).
- Yoon, C. E., Yoshimitsu, N., Ellsworth, W. L. & Beroza, G. C. Foreshocks and mainshock nucleation

- of the 1999 $M_{\rm w}$ 7.1 Hector Mine, California, earthquake. J. Geophys. Res. Solid Earth 124, 1569–1582 (2019).
- Dieterich, J. H. Earthquake nucleation on faults with rate-and state-dependent strength. *Tectonophysics* 211, 115–134 (1992).
- Ohnaka, M. Nonuniformity of the constitutive law parameters for shear rupture and quasistatic nucleation to dynamic rupture: A physical model of earthquake generation processes. *Proc. Natl Acad.* Sci. USA 93, 5795–3802 (1996).
- Tape, C. et al. Earthquake nucleation and fault slip complexity in the lower crust of central Alaska. Nat. Geosci. 11, 536–541 (2018)
- Lockner, D. A., Byerlee, J. D., Kuksenkot, V., Ponomarev, A. & Sidorin, A. Quasi-static fault growth and shear fracture energy in granite. *Nature* 350, 39–42 (1991).

REVIEWS

- Lyakhovsky, V., Ben-Zion, Y. & Agnon, A. Distributed damage, faulting, and friction. J. Geophys. Res. Solid Earth 102, 27635–27649 (1997).
- Renard, F. et al. Volumetric and shear processes in crystalline rock approaching faulting. *Proc. Natl Acad.* Sci. USA 116, 16234–16239 (2019).
- Zaliapin, I. & Ben-Zion, Y. Earthquake clusters in southern California I: Identification and stability.
 J. Geophys. Res. Solid Earth 118, 2847–2864 (2013)
- Zaliapin, I. & Ben-Zion, Y. A global classification and characterization of earthquake clusters. *Geophys. J. Int.* 207, 608–634 (2016).
- Dodge, D. A., Beroza, G. C. & Ellsworth, W. L. Detailed observations of California foreshock sequences: Implications for the earthquake initiation process. *J. Geophys. Res. Solid Earth* 101, 22371–22392 (1996)
- Bouchon, M., Durand, V., Marsan, D., Karabulut, H. & Schmittbuhl, J. The long precursory phase of most large interplate earthquakes. *Nat. Geosci.* 6, 299–302 (2013).
- Wu, C., Meng, X., Peng, Z. & Ben-Zion, Y. Lack of spatiotemporal localization of foreshocks before the 1999 M_w 7.1 Düzce, Turkey, earthquake. *Bull. Seismol.* Soc. Am. 104, 560–566 (2014).
- Tamaribuchi, K., Yagi, Y., Enescú, B. & Hirano, S. Characteristics of foreshock activity inferred from the JMA earthquake catalog. *Earth Planets Space* 70, 90 (2018).
- Abercrombie, R. E. & Mori, J. Occurrence patterns of foreshocks to large earthquakes in the western United States. *Nature* 381, 303–307 (1996).
- Mignan, A. The debate on the prognostic value of earthquake foreshocks: A meta-analysis. Sci. Rep. 4, 4099 (2014).
- Wesnousky, S. G. Seismological and structural evolution of strike-slip faults. *Nature* 335, 22–25 (1988).
- Ben-Zion, Y. & Sammis, C. G. Characterization of fault zones. Pure Appl. Geophys. 160, 677–715 (2003).
- Peng, S. & Johnson, A. M. Crack growth and faulting in cylindrial specimens of Chelmsford granite. *Int. J. Rock Mech. Min. Sci. Geomech. Abstr.* 9, 37–86 (1972).
- Kato, A. & Ueda, T. Source fault model of the 2018 M_w 5.6 northern Osaka earthquake, Japan, inferred from the aftershock sequence. Earth Planets Space 71, 11 (2019).
- 31. Scholz, C. H. *The Mechanics of Earthquakes and Faulting* (Cambridge Univ. Press, 2019).
- Schrank, C. E., Boutelier, D. A. & Cruden, A. R. The analogue shear zone: From rheology to associated geometry. *J. Struct. Geol.* 30, 177–193 (2008).
 Ritter, M. C., Santimano, T., Rosenau, M., Leever, K. &
- Ritter, M. C., Santimano, T., Rosenau, M., Leever, K. & Oncken, O. Sandbox rheometry: Co-evolution of stress and strain in Riedel- and Critical Wedge-experiments. *Tectonophysics* 722, 400–409 (2018).
- Stanchits, S., Vinciguerra, S. & Dresen, G. Ultrasonic velocities, acoustic emission characteristics and crack damage of basalt and granite. *Pure Appl. Geophys.* 163, 974–993 (2006).
- Aben, F. M., Brantut, N., Mitchell, T. M. & David, E. C. Rupture energetics in crustal rock from laboratoryscale seismic tomography. *Geophys. Res. Lett.* 46, 7337–7344 (2019).
- Lyakhovsky, V., Ben-Zion, Y. & Agnon, A. Earthquake cycle, fault zones, and seismicity patterns in a rheologically layered lithosphere. J. Geophys. Res. Solid Earth 106, 4103–4120 (2001).
- Lyakhovsky, V. & Ben-Zion, Y. Evolving geometrical and material properties of fault zones in a damage rheology model. *Geochem. Geophys. Geosyst.* 10, Q11011 (2009).
- Zeng, Y., Petersen, M. D. & Shen, Z. K. Earthquake potential in California-Nevada implied by correlation of strain rate and seismicity. *Geophys. Res. Lett.* 45, 1778–1785 (2018).
- Nishimura, T. Strain concentration zones in the Japanese Islands clarified from GNSS data and its relation with active faults and inland earthquakes. Active Fault Res. 2017, 33–39 (2017).
- Ben-Zion, Y. & Zaliapin, I. Spatial variations of rock damage production by earthquakes in southern California. *Earth Planet. Sci. Lett.* **512**, 184–193 (2019).
- Hauksson, E., Yang, W. & Shearer, P. M. Waveform relocated earthquake catalog for Southern California (1981 to June 2011). *Bull. Seismol. Soc. Am.* 102, 2239–2244 (2012).
- Reches, Z. Mechanisms of slip nucleation during earthquakes. *Earth Planet. Sci. Lett.* 170, 475–486 (1999)

- Nakatani, M. & Scholz, C. H. Frictional healing of quartz gouge under hydrothermal conditions: 1.
 Experimental evidence for solution transfer healing mechanism. J. Geophys. Res. Solid Earth 109, B07201 (2004).
- Aben, F. M., Doan, M. L., Gratier, J. P. & Renard, F. Experimental postseismic recovery of fractured rocks assisted by calcite sealing. *Geophys. Res. Lett.* 44, 7228–7238 (2017).
- Craig, T. J., Chanard, K. & Calais, E. Hydrologicallydriven crustal stresses and seismicity in the New Madrid Seismic Zone. *Nat. Commun.* 8, 2143 (2017)
- Chen, X. & Shearer, P. M. California foreshock sequences suggest aseismic triggering process. *Geophys. Res. Lett.* 40, 2602–2607 (2013).
- Shelly, D. R. A high-resolution seismic catalog for the initial 2019 Ridgecrest earthquake sequence: Foreshocks, aftershocks, and faulting complexity. Seismol. Res. Lett. 91, 1971–1978 (2020).
- Imanishi, K. & Uchide, T. Non-self-similar source property for microforeshocks of the 2014 M₂ 6.2 Northern Nagano, central Japan, earthquake. Geophus. Res. Lett. 44, 5401–5410 (2017).
- Hayashida, Y., Matsumoto, S., Iio, Y., Sakai, S. & Kato, A. Non-double-couple microearthquakes in the focal area of the 2000 Western Tottori earthquake (M 7.3) via hyperdense seismic observations. *Geophus. Res. Lett.* 47, e2019GL084841 (2020).
- Kato, A., Fukuda, J., Nakagawa, S. & Obara, K. Foreshock migration preceding the 2016 M_n7.0 Kumamoto earthquake, Japan. Geophys. Res. Lett. 43, 8945–8953 (2016).
- Ito, Y., Obara, K., Shiomi, K., Sekine, S. & Hirose, H. Slow earthquakes coincident with episodic tremors and slow slip events. *Science* 315, 503–506 (2007).
- Matsuzawa, T., Asano, Y. & Obara, K. Very low frequency earthquakes off the Pacific coast of Tohoku, Japan. Geophys. Res. Lett. 42, 4318–4325 (2015).
- Kaneko, Y., Nielsen, S. B. & Carpenter, B. M. The onset of laboratory earthquakes explained by nucleating rupture on a rate-and-state fault. J. Geophys. Res. Solid Earth 121, 6071–6091 (2016)
- Peng, Z. & Gomberg, J. An integrated perspective of the continuum between earthquakes and slow-slip phenomena. *Nat. Geosci.* 3, 599–607 (2010).
- Obara, K. & Kato, A. Connecting slow earthquakes to huge earthquakes. Science 353, 253–257 (2016).
- Bürgmann, R. The geophysics, geology and mechanics of slow fault slip. Earth Planet. Sci. Lett. 495, 112–134 (2018).
- Veedu, D. M. & Barbot, S. The Parkfield tremors reveal slow and fast ruptures on the same asperity. *Nature* 532, 361–365 (2016).
- Kato, A. et al. Propagation of slow slip leading up to the 2011 M_w 9.0 Tohoku-Oki earthquake. Science 335, 705–708 (2012).
- Miyazaki, S., McGuire, J. J. & Segall, P. Seismic and aseismic fault slip before and during the 2011 off the Pacific coast of Tohoku Earthquake. Earth Planets Space 63, 637–642 (2011).
- Ito, Y. et al. Episodic slow slip events in the Japan subduction zone before the 2011 Tohoku-Oki earthquake. *Tectonophysics* 600, 14–26 (2013).
- Bedford, J. R. et al. Months-long thousand-kilometrescale wobbling before great subduction earthquakes. *Nature* 580, 628–635 (2020).
- Ozawa, S. et al. Preceding, coseismic, and postseismic slips of the 2011 Tohoku earthquake, Japan.
 J. Geophys. Res. Solid Earth 117, B07404 (2012).
- Panet, I., Bonvalot, S., Narteau, C., Remy, D. & Lemoine, J. M. Migrating pattern of deformation prior to the Tohoku-Oki earthquake revealed by GRACE data. Nat. Geosci. 11, 367–373 (2018).
- Ando, R. & Imanishi, K. Possibility of M_w 9.0 mainshock triggered by diffusional propagation of after-slip from M_w 7.3 foreshock. *Earth Planets Space* 63, 767–771 (2011).
- 63, 767–771 (2011).
 Obara, K. Phenomenology of deep slow earthquake family in southwest Japan: Spatiotemporal characteristics and segmentation. *J. Geophys. Res. Solid Earth* 115, B00A25 (2010).
- Igarashi, T. Spatial changes of inter-plate coupling inferred from sequences of small repeating earthquakes in Japan. *Geophys. Res. Lett.* 37, L20304 (2010).
- Chen, T. & Lapusta, N. Scaling of small repeating earthquakes explained by interaction of seismic and aseismic slip in a rate and state fault model. *J. Geophys.* Res. Solid Earth 114, B01311 (2009).
- Uchida, N. & Bürgmann, R. Repeating earthquakes. Annu. Rev. Earth Planet. Sci. 47, 305–332 (2019).

- Ohta, Y. et al. Geodetic constraints on afterslip characteristics following the March 9, 2011, Sanriku-oki earthquake, Japan. *Geophys. Res. Lett.* 39, L16304 (2012).
- Hino, R. et al. Was the 2011 Tohoku-Oki earthquake preceded by aseismic preslip? Examination of seafloor vertical deformation data near the epicenter. *Mar. Geophys. Res.* 35, 181–190 (2014).
- Katakami, S. et al. Spatiotemporal variation of tectonic tremor activity before the Tohoku-Oki earthquake. J. Geophys. Res. Solid Earth 123, 9676–9688 (2018).
- Wang, L. & Burgmann, R. Statistical significance of precursory gravity changes before the 2011 M_w 9.0 Tohoku-Oki earthquake. *Geophys. Res. Lett.* 46, 7323–7332 (2019).
- Bouchon, M. et al. Potential slab deformation and plunge prior to the Tohoku, Iquique and Maule earthquakes. Nat. Geosci. 9, 380–383 (2016).
- Mavrommatis, A. P., Segall, P., Uchida, N. & Johnson, K. M. Long-term acceleration of aseismic slip preceding the M_w 9 Tohoku-oki earthquake: Constraints from repeating earthquakes. *Geophys. Res. Lett.* 42, 9717–9725 (2015).
- Yokota, Y. & Koketsu, K. A very long-term transient event preceding the 2011 Tohoku earthquake. Nat. Commun. 6, 5934 (2015).
- Nat. Commun. 6, 5934 (2015).
 Uchida, N. & Matsuzawa, T. Pre- and postseismic slow slip surrounding the 2011 Tohoku-oki earthquake rupture. Earth Planet. Sci. Lett. 374, 81–91 (2013).
- Baba, S., Takeo, A., Obara, K., Matsuzawa, T. & Maeda, T. Comprehensive detection of very low frequency earthquakes off the Hokkaido and Tohoku Pacific coasts, northeastern Japan. J. Geophys. Res. Solid Earth 125, e2019JB017988 (2020).
- Sato, T., Hiratsuka, S. & Mori, J. Precursory seismic activity surrounding the high-slip patches of the 2011 Mw 9.0 Tohoku-Oki earthquake. *Bull. Seismol. Soc. Am.* 103, 3104–3114 (2013).
- Kato, A. & Nakagawa, S. Multiple slow-slip events during a foreshock sequence of the 2014 Iquique, Chile M., 8.1 earthquake. Geophys. Res. Lett. 41, 5420–5427 (2014)
- Ruiz, S. et al. Intense foreshocks and a slow slip event preceded the 2014 Iquique M_w8.1 earthquake. *Science* 1165, 1165–1169 (2014).
- Schurr, B. et al. Gradual unlocking of plate boundary controlled initiation of the 2014 Iquique earthquake. Nature 512, 299–302 (2014).
- Kato, A., Fukuda, J., Kumazawa, T. & Nakagawa, S. Accelerated nucleation of the 2014 Iquique, Chile Mw 8.2 earthquake. Sci. Rep. 6, 24792 (2016).
- 84. Bedford, J., Moreno, M., Schurr, B., Bartsch, M. & Oncken, O. Investigating the final seismic swarm before the Iquique-Pisagua 2014 M_w 8.1 by comparison of continuous GPS and seismic foreshock data. *Geophys. Res. Lett.* 42, 3820–3828 (2015).
- Herman, M. W., Furlong, K. P., Hayes, G. P. & Benz, H. M. Foreshock triggering of the 1 April 2014 Mw 8.2 Iquique, Chile, earthquake. Earth Planet. Sci. Lett. 447, 119–129 (2016).
- Jara, J., Socquet, A., Marsan, D. & Bouchon, M. Long-term interactions between intermediate depth and shallow seismicity in North Chile subduction zone. *Geophys. Res. Lett.* 44, 9283–9292 (2017).
- Socquet, A. et al. An 8 month slow slip event triggers progressive nucleation of the 2014 Chile megathrust. Geophys. Res. Lett. 44, 4046–4053 (2017).
- Ruiz, S. et al. Nucleation phase and dynamic inversion of the M_n 6.9 Valparaiso 2017 earthquake in Central Chile. Geophys. Res. Lett. 44, 10,290–10,297
- 89. Nishikawa, T. & Ide, S. Recurring slow slip events and earthquake nucleation in the source region of the M 7 Ibaraki-Oki earthquakes revealed by earthquake swarm and foreshock activity. J. Geophys. Res. Solid Earth 123, 7950–7968 (2018).
- Reches, Z., Zu, X. & Carpenter, B. M. Energy-flux control of the steady-state, creep, and dynamic slip modes of faults. Sci. Rep. 9, 10627 (2019).
- Frank, W. B., Rousset, B., Lasserre, C. & Campillo, M. Revealing the cluster of slow transients behind a large slow slip event. Sci. Adv. 4, eaat0661 (2018).
- Bartlow, N. M. A long-term view of episodic tremor and slip in Cascadia. *Geophys. Res. Lett.* 47, e2019GL085303 (2020).
- Wallace, L. M. Slow slip events in New Zealand. Annu. Rev. Earth Planet. Sci. 48, 175–203 (2020).

- Yokota, Y. & Ishikawa, T. Shallow slow slip events along the Nankai Trough detected by GNSS-A. Sci. Adv. 6, eaay5786 (2020).
- Kano, M. & Kato, A. Detailed spatial slip distribution for short-term slow slip events along the Nankai subduction zone, southwest Japan. J. Geophys. Res. Solid Earth 125, e2020JB019613 (2020).
 Mazzotti, S. & Adams, J. Variability of near-term
- Mazzotti, S. & Adams, J. Variability of near-term probability for the next great earthquake on the Cascadia subduction zone. *Bull. Seismol. Soc. Am.* 94, 1954–1959 (2004)
- 1954–1959 (2004). 97. Kano, M., Kato, A. & Obara, K. Episodic tremor and slip silently invades strongly locked megathrust in the Nankai Trough. *Sci. Rep.* **9**, 9270 (2019).
- Dixon, T. H. et al. Earthquake and tsunami forecasts: Relation of slow slip events to subsequent earthquake rupture. Proc. Natl Acad. Sci. USA 111, 17039–17044 (2014).
- Graham, S. E. et al. GPS constraints on the 2011–2012 Oaxaca slow slip event that preceded the 2012 March 20 Ometepec earthquake, southern Mexico. Geophys. J. Int. 197, 1593–1607 (2014).
- 100. Radiguet, M. et al. Triggering of the 2014 M_w7.3 Papanoa earthquake by a slow slip event in Guerrero, Mexico. Nat. Geosci. 9, 829–833 (2016).
- 101. Hirose, H., Kimura, H., Enescu, B. & Aoi, S. Recurrent slow slip event likely hastened by the 2011 Tohoku earthquake. *Proc. Natl Acad. Sci. USA* 109, 15157–15161 (2012).
- 102. Vallée, M. et al. Întense interface seismicity triggered by a shallow slow slip event in the Central Ecuador subduction zone. J. Geophys. Res. Solid Earth 118, 2965–2981 (2013).
- 103. Bartlow, N. M., Wallace, L. M., Beavan, R. J., Bannister, S. & Segall, P. Time-dependent modeling of slow slip events and associated seismicity and tremor at the Hikurangi subduction zone, New Zealand. J. Geophys. Res. Solid Earth 119, 734–753 (2014).
- 104. Hirose, H., Matsuzawa, T., Kimura, T. & Kimura, H. The Boso slow slip events in 2007 and 2011 as a driving process for the accompanying earthquake swarm. Geophys. Res. Lett. 41, 2778–2785 (2014)
- 105. Fukuda, J. Variability of the space-time evolution of slow slip events off the Boso Peninsula, Central Japan, from 1996 to 2014. J. Geophys. Res. Solid Earth 123, 732–760 (2018).
- 106. Fukuda, J., Kato, A., Obara, K., Miura, S. & Kato, T. Imaging of the early acceleration phase of the 2013–2014 Boso slow slip event. *Geophys. Res. Lett.* 41, 7493–7500 (2014).
- 107. Kato, A., Igarashi, T. & Óbara, K. Detection of a hidden Boso slow slip event immediately after the 2011 M_w 9.0 Tohoku-Oki earthquake, Japan. *Geophys. Res. Lett.* 41, 5868–5874 (2014).
- 108. Fukuda, J., Kato, A., Kato, N. & Aoki, Y. Are the frictional properties of creeping faults persistent? Evidence from rapid afterslip following the 2011 Tohoku-oki earthquake. Geophys. Res. Lett. 40, 3613–3617 (2013).
- 109. Hatakeyama, N., Uchida, N., Matsuzawa, T. & Nakamura, W. Emergence and disappearance of interplate repeating earthquakes following the 2011 M9.0 Tohoku-oki earthquake: Slip behavior transition between seismic and aseismic depending on the loading rate. J. Geophys. Res. Solid Earth 122, 5160–5180 (2017).
- Scholz, C. H. Earthquakes and friction laws. *Nature* 391, 37–42 (1998).
 Lay, T. et al. Depth-varying rupture properties of
- Lay, T. et al. Depth-varying rupture properties of subduction zone megathrust faults. J. Geophys. Res. Solid Earth 117, B04311 (2012).
- 112. Guérin-Marthe, S., Nielsen, S., Bird, R., Giani, S. & Di Toro, G. Earthquake nucleation size: Evidence of loading rate dependence in laboratory faults. J. Geophys. Res. Solid Earth 124, 689–708 (2019).
- 113. Rolandone, F., Bürgmann, R. & Nadeau, R. M. The evolution of the seismic-aseismic transition during the earthquake cycle: Constraints from the time-dependent depth distribution of aftershocks. Geophys. Res. Lett. 31, L23610 (2004).
- 114. Ben-Zion, Y. & Lyakhovsky, V. Analysis of aftershocks in a lithospheric model with seismogenic zone

- governed by damage rheology. *Geophys. J. Int.* **165**, 197–210 (2006).
- 115. Cheng, Y. & Ben-Zion, Y. Transient brittle-ductile transition depth induced by moderate-large earthquakes in southern and Baja California. *Geophys. Res. Lett.* 46, 11109–11117 (2019).
- 116. Jamtveit, B., Ben-Zion, Y., Renard, F. & Austrheim, H. Earthquake-induced transformation of the lower crust. *Nature* 556, 487–491 (2018).
- 117. Kato, N., Yamamoto, K., Yamamoto, H. & Hirasawa, T. Strain-rate effect on frictional strength and the slip nucleation process. *Tectonophysics* 211, 269–282 (1992).
- Mclaskey, G. C. & Yamashita, F. Slow and fast ruptures on a laboratory fault controlled by loading characteristics. J. Geophys. Res. Solid Earth 122, 3719–3738 (2017).
- 119. Xu, S. et al. Strain rate effect on fault slip and rupture evolution: Insight from meter-scale rock friction experiments. *Tectonophysics* 733, 209–231 (2018).
- McLaskey, G. C. Earthquake initiation from laboratory observations and implications for foreshocks.
 J. Geophys. Res. Solid Earth 124, 12882–12904 (2019).
- Okubó, P. G. & Dieterich, J. H. Effects of physical fault properties on frictional instabilities produced on simulated faults. *J. Geophys. Res.* 89, 5817–5827 (1984).
- 122. Ohnaka, M. & Shen, L. Scaling of the shear rupture process from nucleation to dynamic propagation: Implications of geometric irregularity of the rupturing surfaces. J. Geophys. Res. Solid Earth 104, 817–844 (1999).
- 123. Marone, C. & Kilgore, B. Scaling of the critical slip distance for seismic faulting with shear strain in fault zones. *Nature* 362, 618–621 (1993).
- 124. Harbord, C. W. A., Nielsen, S. B., De Paola, N. & Holdsworth, R. E. Earthquake nucleation on rough faults. *Geology* 45, 931–934 (2017).
- 125. McLaskey, G. C. & Kilgore, B. D. Foreshocks during the nucleation of stick-slip instability. *J. Geophys. Res. Solid Earth* 118, 2982–2997 (2013).
- 126. Shibazaki, B. & Matsu'ura, M. Foreshocks and pre-events associated with the nucleation of large earthquakes. *Geophys. Res. Lett.* 22, 1305–1308 (1995)
- 127. Ben-Zion, Y. & Rice, J. R. Dynamic simulations of slip on a smooth fault in an elastic solid. *J. Geophys. Res. Solid Earth* **102**, 17771–17784 (1997).
- Uenishi, K. & Rice, J. R. Universal nucleation length for slip-weakening rupture instability under nonuniform fault loading. J. Geophys. Res. Solid Earth 108, 2042 (2003).
- 129. Acosta, M., Passelègue, F. X., Schubnel, A., Madariaga, R. & Violay, M. Can precursory moment release scale with earthquake magnitude? A view from the laboratory. *Geophys. Res. Lett.* 46, 12927–12937 (2019).
- Mclaskey, G. C. & Lockner, D. Preslip and cascade processes initiating laboratory stick slip. *J. Geophys.* Res. Solid Earth 119, 6323–6336 (2014).
- Passelègue, F. X. et al. in Fault Zone Dynamic Processes: Evolution of Fault Properties During Seismic Rupture Ch. 12 (eds Thomas, M. Y., Mitchell, T. M. & Bhat, H. S.) (Wiley, 2017).
- 132. Chu, R. et al. Initiation of the great M_w 9.0 Tohoku–Oki earthquake. *Earth Planet. Sci. Lett.* 308, 277–283 (2011).
- 133. Ohnaka, M. A physical scaling relation between the size of an earthquake and its nucleation zone size. Pure Appl. Geophys. 157, 2259–2282 (2000).
- 134. Ide, S. & Aochi, H. Earthquakes as multiscale dynamic ruptures with heterogeneous fracture surface energy. J. Geophys. Res. Solid Earth 110, B11303 (2005).
- 135. Hori, T. & Miyazaki, S. A possible mechanism of M 9 earthquake generation cycles in the area of repeating M 7 ~ 8 earthquakes surrounded by aseismic sliding. Earth Planets Space 63, 773–777 (2011).
- 136. Noda, H., Nakatani, M. & Hori, T. Large nucleation before large earthquakes is sometimes skipped due to cascade-up—Implications from a rate and state simulation of faults with hierarchical asperities.

- J. Geophys. Res. Solid Earth 118, 2924–2952 (2013).
- Ökubó, K. et al. Dynamics, radiation, and overall energy budget of earthquake rupture with coseismic off-fault damage. *J. Geophys. Res. Solid Earth* 124, 11771–11801 (2019).
- 138. Kurzon, I., Lyakhovsky, V. & Ben-Zion, Y. Dynamic rupture and seismic radiation in a damage–breakage rheology model. *Pure Appl. Geophys.* **176**, 1003–1020 (2019).
- Dieterich, J. H. & Kilgore, B. D. Imaging surface contacts: Power law contact distributions and contact stresses in quartz, calcite, glass and acrylic plastic. *Tectonophysics* 256, 219–239 (1996).
- 140. Muhuri, S. K., Dewers, T. A., Scott, T. E. Jr & Reches, Z. Interseismic fault strengthening and earthquake-slip instability: Friction or cohesion? *Geology* 31, 881–884 (2003).
- Yu, W. C., Song, T. R. A. & Silver, P. G. Temporal velocity changes in the crust associated with the great Sumatra earthquakes. *Bull. Seismol. Soc. Am.* 103, 2797–2809 (2013).
 Pei, S. et al. Seismic velocity reduction and
- 142. Pei, S. et al. Seismic velocity reduction and accelerated recovery due to earthquakes on the Longmenshan fault. *Nat. Geosci.* 12, 387–392 (2019).
- 143. Qiu, H., Hillers, G. & Ben-Zion, Y. Temporal changes of seismic velocities in the San Jacinto Fault zone associated with the 2016 M_w, 5.2 Borrego Springs earthquake. *Geophys. J. Int.* 220, 1536–1554 (2020).
- 144. Ben-Zion, Y. A critical data gap in earthquake physics. *Seismol. Res. Lett.* **90**, 1721–1722 (2019).
- 145. Kong, Q. et al. Machine learning in seismology: Turning data into insights. Seismol. Res. Lett. 90, 3–14 (2019).
- 146. Bergen, K. J., Johnson, P. A., De Hoop, M. V. & Beroza, G. C. Machine learning for data-driven discovery in solid Earth geoscience. *Science* 363, eaau0323 (2019).
- 147. McBeck, J., Aiken, J. M., Ben-Zion, Y. & Renard, F. Predicting the proximity to macroscopic failure using local strain populations from dynamic in situ X-ray tomography triaxial compression experiments on rocks. Earth Planet. Sci. Lett. 543, 116344 (2020).
- 148. Zaliapin, I. & Ben-Zion, Y. Earthquake declustering using the nearest-neighbor approach in space-timemagnitude domain. J. Geophys. Res. Solid Earth 125, e2018JB017120 (2020).
- 149. Hayes, G. P. et al. Continuing megathrust earthquake potential in Chile after the 2014 Iquique earthquake. *Nature* 512, 295–298 (2014).

Acknowledgements

The authors are grateful to I. Zaliapin for helping to produce Figs 1,2, R. Hino for providing seafloor-level data, J. Fukuda for contributing Fig. 5 and S. Guérin-Marthe for contributing Fig. 6. They acknowledge support by JSPS KAKENHI grant number JP16H06473, JST CREST grant number JPMJCR1763, Earthquake and Volcano Hazards Observation and Research Program in MEXT, the US National Science Foundation (grant EAR-1722561) and the Southern California Earthquake Center (based on NSF Cooperative Agreement EAR-1600087 and USGS Cooperative Agreement G17AC00047).

Author contributions

 $\mbox{A.K.}$ and $\mbox{Y.B.-Z.}$ both discussed the outline of the Review and wrote the article together.

Competing interests

The authors declare no competing interests.

Peer review information

Nature Reviews Earth & Environment thanks Ze'ev Reches and the other, anonymous, reviewer(s) for their contribution to the peer review of this work.

Publisher's note

Springer Nature remains neutral with regard to jurisdictional claims in published maps and institutional affiliations.

© Springer Nature Limited 2020, corrected publication 2021